

Intra-Atrial Dyssynchrony Using Cardiac Magnetic Resonance to Quantify Tissue Remodeling in Patients with Atrial Fibrillation

Luisa Allen Ciuffo,^{1,2} João Lima,³ Henrique Doria de Vasconcellos,² Muhammad Balouch,² Susumu Tao,² Saman Nazarian,² David D. Spragg,² Joseph E. Marine,² Ronald D. Berger,² Hugh Calkins,² Hiroshi Ashikaga²

University of New Mexico,¹ New Mexico – USA

The Johns Hopkins University,² Baltimore – USA

Johns Hopkins Hospital and Health System,³ Baltimore – USA

Abstract

Background: Recent studies suggest that left atrial (LA) late gadolinium enhancement (LGE) can quantify the underlying tissue remodeling that harbors atrial fibrillation (AF). However, quantification of LA-LGE requires labor-intensive magnetic resonance imaging acquisition and postprocessing at experienced centers. LA intra-atrial dyssynchrony assessment is an emerging imaging technique that predicts AF recurrence after catheter ablation. We hypothesized that 1) LA intra-atrial dyssynchrony is associated with LA-LGE in patients with AF and 2) LA intra-atrial dyssynchrony is greater in patients with persistent AF than in those with paroxysmal AF.

Method: We conducted a cross-sectional study comparing LA intra-atrial dyssynchrony and LA-LGE in 146 patients with a history of AF (60.0 ± 10.0 years, 30.1% nonparoxysmal AF) who underwent pre-AF ablation cardiac magnetic resonance (CMR) in sinus rhythm. Using tissue-tracking CMR, we measured the LA longitudinal strain in two- and four-chamber views. We defined intra-atrial dyssynchrony as the standard deviation (SD) of the time to peak longitudinal strain (SD-TPS, in %) and the SD of the time to the peak pre-atrial contraction strain corrected by the cycle length (SD-TPS_{preAF}, in %). We used the image intensity ratio (IIR) to quantify LA-LGE.

Results: Intra-atrial dyssynchrony analysis took 5 ± 9 minutes per case. Multivariable analysis showed that LA intra-atrial dyssynchrony was independently associated with LA-LGE. In addition, LA intra-atrial dyssynchrony was significantly greater in patients with persistent AF than those with paroxysmal AF. In contrast, there was no significant difference in LA-LGE between patients with persistent and paroxysmal AF. LA intra-atrial dyssynchrony showed excellent reproducibility and its analysis was less time-consuming (5 ± 9 minutes) than the LA-LGE (60 ± 20 minutes).

Conclusion: LA Intra-atrial dyssynchrony is a quick and reproducible index that is independently associated with LA-LGE to reflect the underlying tissue remodeling. (Arq Bras Cardiol. 2019; 112(4):441-450)

Keywords: Heart Atria; Atrial Fibrillation; Diagnostic Imaging; Echocardiography/methods; Magnetic Resonance Spectroscopy.

Introduction

Atrial fibrillation (AF) is the most prevalent arrhythmia¹ and an independent predictor of stroke² and dementia.³ The cornerstone treatment for drug-refractory AF is invasive catheter ablation with pulmonary vein isolation (PVI), but the rate of recurrence after PVI is relatively high.⁴ Preprocedural assessment of left atrial (LA) late gadolinium enhancement (LGE) is a predictor of AF recurrence after PVI.^{5,6} LA-LGE can be considered as a surrogate for the underlying tissue remodeling represented by fibrotic replacement that promotes AF. Although LA-LGE has a potential to improve the clinical outcomes of PVI by refining patient selection, its major limitation is the

requirement of labor-intensive magnetic resonance imaging (MRI) acquisition and postprocessing, which are not always compatible with clinical workflow. In addition, LA-LGE requires intravenous contrast administration, which is contraindicated in subgroups of PVI candidates, such as individuals with renal failure or allergic reactions to gadolinium-based contrast materials. As a result, LA-LGE is not part of the standard clinical practice, except at experienced centers.⁷

Recently, we demonstrated that preprocedural assessment of LA intra-atrial dyssynchrony predicts AF recurrence after PVI.⁸ The assessment utilizes a tissue-tracking technology that can be applied to any routinely acquired cine MRI, which does not require intravenous contrast administration.⁹ It is simple and quick, only based on two long-axis views (two-chamber and four-chamber views) of routine cine MRI. Because the LA structure and function reflect the underlying tissue fibrosis,¹⁰ it is possible that LA intra-atrial dyssynchrony serves as a surrogate for LA-LGE.

In this study, we hypothesized that LA intra-atrial dyssynchrony is associated with LA-LGE in patients with AF. In addition, we further hypothesized that LA intra-atrial dyssynchrony is greater in patients with persistent AF than

Mailing Address: Luisa Allen Ciuffo •

University of New Mexico, 2211. 87131-1466, Lomas Blvd NE Albuquerque, Novo México – USA

E-mail: iallem@hotmail.com

Manuscript received October 21, 2018, revised manuscript January 05, 2019, accepted January 21, 2019

DOI: 10.5935/abc.20190064

in those with paroxysmal AF. To test these hypotheses, we conducted a cross-sectional study to evaluate LA intra-atrial dyssynchrony and LA-LGE in patients with either paroxysmal or persistent AF. We also quantified the amount of time required for the postprocessing, and the inter-reader and intra-reader reproducibility of LA intra-atrial dyssynchrony.

Methods

Study population

The study included 146 consecutive patients with symptomatic, drug-refractory AF referred for catheter ablation at the Johns Hopkins Hospital between June 2010 and December 2015 who underwent pre-procedural cardiac magnetic resonance (CMR). Patients with prior AF ablation or surgical procedure in the LA were excluded. Based on Heart Rhythm Society most recent guidelines, paroxysmal AF was defined as AF that terminates spontaneously or with intervention within 7 days of onset. Persistent AF is defined as continuous AF that is sustained beyond 7 days.⁷ Patients in AF at the time of CMR were also excluded. The protocol was approved by the Institutional Review Board of The Johns Hopkins Hospital, and all the patients provided written informed consent.

CMR protocol

CMR was performed with a 1.5-Tesla scanner (Avanto; Siemens Medical Systems, Erlangen, Germany), a 6-channel phased-array body coil in combination with a 6-channel spine matrix coil. Electrocardiogram (ECG)-gated, breath-holding cine CMR images were acquired in the long-axis two- and four-chamber views by true fast imaging with steady-state precession (TrueFISP) sequence with the following parameters: TE/TR 3.0/1.5 ms; flip angle 78°; in-plane pixel size 1.5×1.5 mm²; slice thickness 8 mm; slice spacing 2 mm; 30 frames per ECG R-R interval with a temporal resolution of 20-40 ms. The patients also underwent respiratory-navigated, ECG-gated LGE for quantification of LA fibrosis (Figure 3). LGE images were acquired within 15-25 minutes following the injection of gadopentetate dimeglumine (0.2 mmol/kg; Bayer Healthcare Pharmaceuticals, Montville, NJ, USA) using a fat-saturated 3D inversion recovery-prepared fast spoiled gradient-recalled echo sequence with the following parameters: TE/TR 1.52/3.8 ms; flip angle 10°; in-plane pixel size 1.3×1.3 mm²; slice thickness 2.0 mm. The trigger time for three-dimensional (3D) LGE images was optimized to acquire imaging data during LA diastole as determined by the cine CMR images. The optimal inversion time was determined by an inversion time scout scan (median 270 ms, range 240-290 ms) to maximize nulling of the LA myocardium. The image intensity ratio (IIR)¹¹ was measured to quantify LA-LGE using QMass MR (version 7.2; Medis Medical Imaging Systems bv, Leiden, the Netherlands) on axial images from 3D axial image data. Briefly, IIR is a signal intensity of LA-LGE normalized by the mean signal intensity of the LA blood pool. The IIR threshold of 1.22 that corresponds to bipolar voltage 0.3 mV on intracardiac electrogram was used to define myocardial fibrosis.^{12,13} Preprocedural CMR scans were acquired within a range of 15–25 minutes (mean 18.8 ± 2.4 minutes).

Magnetic resonance imaging Analysis

Left atrial intra-atrial dyssynchrony

Multimodality Tissue Tracking software (MTT, version 6.1, Toshiba, Japan) was used to quantify the LA longitudinal strains and strain rates in two-chamber and four-chamber views. The accuracy and reproducibility of MTT have been validated previously.^{9,14} Briefly, an experienced operator, blinded to the type of AF, defined the LA endocardial and epicardial borders at the LA end diastole (Figure 1). The confluence of the pulmonary veins and LA appendage were excluded as appropriate. The software automatically propagates endocardial/epicardial borders over the entire cardiac cycle using a template matching algorithm.¹⁴ Finally, the operator verified the quality of the tracking generated by MTT. The software automatically divides the LA into six equal-length segments in each of the two- and four-chamber views, creating a total of 12 segments (Figure 1). Longitudinal strain and strain rate were calculated within each of the 12 segments (Figure 2). Based on those curves, we defined five indices of LA intra-atrial dyssynchrony as follows:^{15,16}

- SD-time to peak strain (SD-TPS): Standard deviation of the time to peak longitudinal strain in 12 segments. This index quantifies intra-atrial dyssynchrony of the LA reservoir function.
- SD-time to peak pre-atrial contraction strain (SD-TPS_{preA}): Standard deviation of the time to the peak pre-atrial contraction strain in 12 segments. This index quantifies intra-atrial dyssynchrony of the LA reservoir and conduit function.

A higher value of each index reflects a greater degree of intra-atrial dyssynchrony. We also present the values of LA dyssynchrony as percentage (SD, %) of R-R' interval. A similar assessment of LA dyssynchrony has been published and validated before using 3D echocardiography against standard two-dimensional (2D) echocardiography, in a population of individuals with paroxysmal and persistent AF against healthy subjects.^{17,18} Out of a total of 1,752 segments, 34 (1.94%) were excluded from analysis because these segments lacked well-defined peaks in the strain/strain rate curves. A total of 22 subjects had at least one segment that was not analyzable, of whom 15 were in the persistent AF group and 7 were in the paroxysmal AF group (p = 0.02).

LA function

LA functional analysis was described previously.¹⁶ The LA longitudinal strain and strain rate were calculated by averaging strain values in all 12 segments obtained in long-axis two- and four-chamber views. A positive and negative strain value indicates stretch and shortening, respectively, with respect to the reference configuration at the ventricular end diastole, defined as the peak of R wave on surface ECG. Maximum LA longitudinal strain (S_{max}) and pre-atrial contraction strain (S_{preA}) were identified from the strain curve (Figure 2); the strain rates in left ventricular (LV) systole (SR_s), LV early diastole (SR_e), and LA contraction (SR_a) were obtained from the strain rate curve. The LA volume curve was generated by the biplane modified

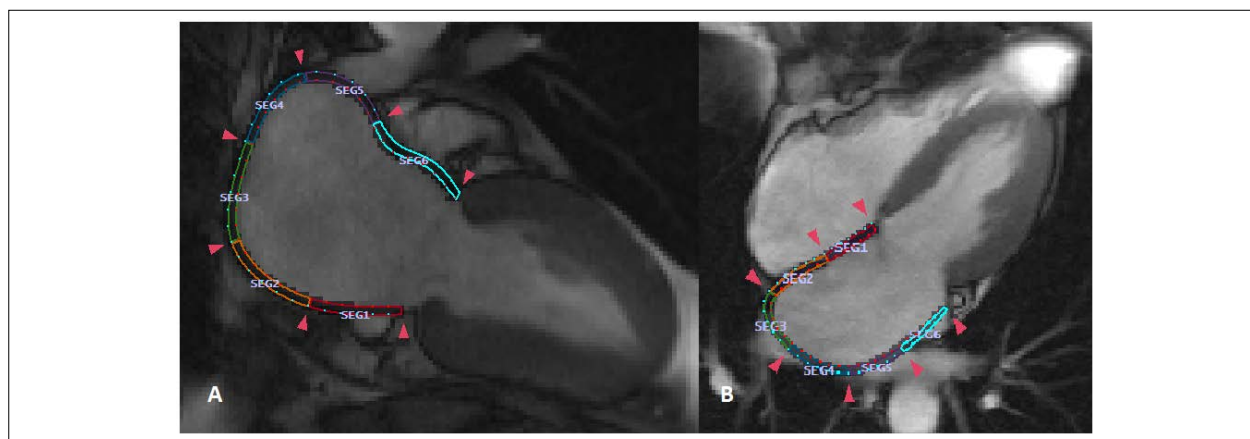


Figure 1 – Quantification of left atrial regional function using cine cardiac magnetic resonance. The figures show a total of 12 color-coded segments within the left atrium. A: Two-chamber view with six equal-length segments; B: Four-chamber view with six equal-length segments.

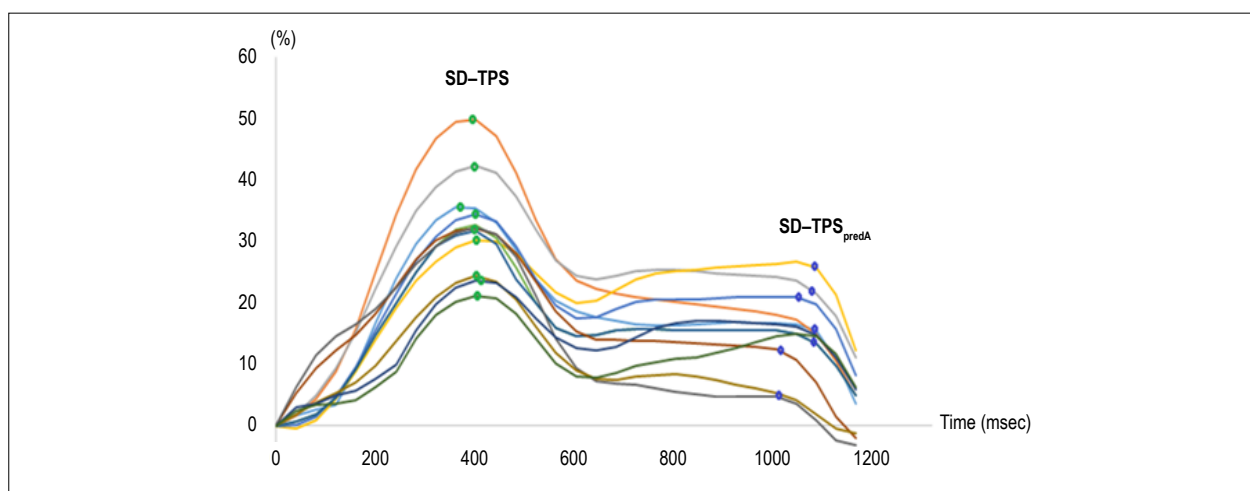


Figure 2 – Strain curves of all 12 segments. Green dots, standard deviation of the time to peak strain (SD-TPS) of each segment; Blue dots, standard deviation of the time to peak pre-atrial strain (SD-TPS_{preA}) of each segment.

Simpson's method, which was validated using the area-length method¹⁹⁻²¹ and the maximum LA volume (V_{max}), pre-atrial contraction LA volume (V_{preA}), and minimum LA volume (V_{min}) were extracted. All LA volumes were normalized by body surface area based on the Haycock's formula.²² The LA emptying fractions (EF) were calculated as follows: LA total EF = $(V_{max} - V_{min}) \times 100\% / V_{max}$; LA passive EF = $(V_{max} - V_{preA}) \times 100\% / V_{max}$; and LA active EF = $(V_{preA} - V_{min}) \times 100\% / V_{preA}$.

Ablation Protocol

PVI catheter ablation of AF was performed using an electroanatomic mapping system with an image integration module (CARTO and CARTOMERGE®, Biosense Webster, Irvine, CA, USA) to merge preprocedural CMR. The electrical isolation of the pulmonary veins was confirmed by a circular multipolar electrode mapping catheter (Lasso, Biosense Webster, Irvine, CA, USA). In cases of persistent AF, the ablation procedure usually included complementary ablation strategies. Ablation was performed with either an open-irrigated

radiofrequency ablation catheter with or without force sensing, or a cryoballoon ablation catheter.

Reproducibility

Intra-reader reproducibility was established by one reader who performed analysis of the 15 studies twice, with an interval of 7 days between the two analyses. Inter-reader reproducibility was assessed by two readers who analyzed the same 15 cases. The second reader was blinded regarding the results of the first reader.

Statistical analysis

Data are presented as mean \pm SD for normally distributed continuous variables, median and interquartile range (IQR) for non-normally distributed continuous variables, and percentages for categorical variables. Comparison between groups was performed using Student's *t* test, chi-square test, and Fisher's exact test, as appropriate. Multivariable linear regression

analysis and Pearson's correlation were also used to examine the relationship between LA intra-atrial dyssynchrony and LA-LGE. Four linear regression models are presented: Model 1 (unadjusted), Model 2 (adjusted for the following clinical characteristics: age, sex, type of AF, body mass index [BMI], history of heart failure, hypertension, and obstructive sleep apnea), and Model 3 (Model 2 + V_{\min} and S_{\max}). Indices of LA intra-atrial dyssynchrony and LA-LGE were log-transformed due to non-normal distribution. We also evaluated the possibility of interaction between LA intra-atrial dyssynchrony and AF type. Pearson's correlation coefficient was categorized with the following correlations: poor, 0; slight, 0.01-0.20; fair, 0.21-0.40; moderate, 0.41-0.60; good, 0.61-0.80, and excellent, 0.81-1.00. In a subset of randomly selected participants (n = 15), a Bland-Altman analysis was performed to quantify intraobserver and interobserver reproducibility and inter-study reproducibility(21)(22) ^{23,24}. Moreover, the intraclass correlation coefficient (ICC) with a two-way random model was evaluated, in which agreement was categorized as follows: ICC, < 0.40, poor; ICC 0.40-0.75, fair to good; and ICC > 0.75, excellent. The statistical computations were performed using Stata, version 12.0 (StataCorp LLC, College Station, TX, USA).

Results

Clinical

A total of 146 patients were included in the final analysis, and their clinical characteristics are summarized in Table 1. There were 61 (29.3%) female patients, and the mean age was 60.0 ± 10.0 years. A total of 102 patients (69.8%) had

paroxysmal AF at the time of the procedure. Patients with paroxysmal and persistent AF were similar in terms of clinical baseline characteristics and medication usage, as demonstrated in Table 1; 4 of 44 patients (9.1%) in the persistent group and 2 of 102 patients (2.0%) in the paroxysmal group underwent cardioversion within 3-4 weeks prior to CMR (p = 0.158).

Left atrial function, intra-atrial dyssynchrony, and atrial fibrillation type

Patients with persistent AF had lower total LA emptying fraction (LAEF), active LAEF, SR, SR_e , SR_a , and left ventricular ejection fraction (LVEF) than those with paroxysmal AF (Table 2). In addition, SD-TPS was significantly higher in patients with persistent AF than in those with paroxysmal AF (median 3.6% versus 2.9 %, respectively, p = 0.036). $SD-TPS_{preA}$ was not significantly different between the AF types (4.6% versus 3.7%, respectively, p = 0.227) (Table 2). The dyssynchrony analysis was performed in a consistent manner in all cases and took 5 ± 9 minutes per case. There was no difference in the amount of time required for the dyssynchrony analysis between the AF types (p = 0.35).

LA Dyssynchrony and LA-LGE

There was no significant difference in the extent of LA fibrosis quantified by LGE between the AF types (11.6 [6-17.6]% of LA surface versus 13.8 [7.6-28.4] % of LA surface in the paroxysmal and persistent AF groups, respectively, p = 0.061). In Model 1, log-transformed SD-TPS and $SD-TPS_{preA}$ were associated with the LA degree of log-transformed LA-LGE enhancement (Table 3). After adjusting for age, sex, BMI, AF type, history of heart failure,

Table 1 – Baseline characteristics

	Overall (n = 146)	Paroxysmal AF (n = 102)	Persistent AF (n = 44)	p
Clinical				
Age, years	60.0 ± 10.0	60.0 ± 10.1	59.7±9.8	0.906
Body mass index, kg/m ²	28.4 ± 5.5	28.0 ± 5.4	29.9 ± 5.3	0.073
Male, n (%)	102 (70.0)	74 (72.5)	28 (63.3)	0.134
Heart failure, n (%)	14 (9.6)	8 (7.8)	6 (13.6)	0.082
Coronary artery disease/vascular disease, n (%)	12 (8.2)	10 (9.8)	2 (4.5)	0.536
Diabetes, n (%)	15 (15.4)	12 (11.8)	3 (6.8)	0.704
Hypertension, n (%)	60 (41.1)	42 (41.2)	18 (40.9)	0.154
History of stroke/TIA, n (%)	9 (6.2)	8 (7.8)	1 (2.3)	0.351
CHA ₂ DS ₂ -VAS _c	1.60 ± 1.5	1.5 ± 1.6	1.6 ± 1.2	0.942
Obstructive sleep apnea, n (%)	23 (15.8)	17 (16.7)	6 (13.6)	0.796
Ablation strategy (cryoablation), n (%)	34 (23.3)	28 (27.5)	6 (13.6)	0.324
Medication				
ACEI/ARBs, n (%)	37 (25.3)	24 (23.5)	13 (29.5)	0.389
Beta-blockers, n (%)	81 (56.3)	62 (60.8)	19 (43.2)	0.788
Calcium-channel blockers, n (%)	33 (22.9)	26 (25.5)	7 (15.9)	0.637
Number of antiarrhythmic drugs	1.2 ± 0.8	1.2 ± 0.8	1.4 ± 0.7	0.108

Data are presented as mean ± standard deviation, n (%), or median. AF: atrial fibrillation; TIA: transient ischemic attack; ACEI/ARB: angiotensin-converting enzyme inhibitor/angiotensin receptor blockers; CHA₂DS₂-VAS_c: score for stroke risk assessment in atrial fibrillation.

Table 2 – Left atrial (LA) functional parameters by groups

	Paroxysmal AF (n = 102)		Persistent AF (n = 44)		p
	Mean	95% CI	Mean	95% CI	
LA structure					
Minimum LA volume index, mm ³ /m ²	19.0 ± 7.8	18.5 – 21.4	23.0 ± 10.1	19.5 – 26.5	0.062
Maximum LA volume index, mm ³ /m ²	38.8 ± 10.5	36.8 – 40.8	39.6 ± 11.7	35.6 – 43.7	0.691
LA Function					
Total LAEF, %	49.5 ± 10.0	47.6 – 51.4	44.0 ± 12.6	39.6 – 48.3	0.008
Passive LAEF, %	22.9 ± 7.3	21.6 – 24.3	20.7 ± 8.3	17.8 – 23.5	0.128
Active LAEF, %	34.6 ± 10.8	32.5 – 36.6	29.5 ± 14.1	24.6 – 34.3	0.026
S _{max} ^l , %	28.9 ± 8.9	27.2 – 30.5	26.0 ± 11.8	22.0 – 30.1	0.132
SR	1.1 ± 0.4	1.1 – 1.2	1.1 ± 0.5	0.9 – 1.3	0.347
SR _e	-1.1 ± 0.5	-1.2 – -1.0	-0.8 ± 0.4	-1.0 – -0.7	0.010
SR _a	-1.4 ± 0.5	-1.5 – -1.3	-1.1 ± 0.6	-1.3 – -0.9	0.011
LVEF, %	58.4 ± 6.0	57.0 – 59.8	53.4 ± 10.3	49.4 – 57.4	0.004
	Median	IQR	Median	IQR	p
Dyssynchrony					
Mean TPS, ms	397.8	374.5 - 420.2	403.5	369.9 - 429.0	0.538
SD-TPS, %	2.9	2.1 – 3.9	3.6	2.3 – 4.9	0.036
Log - SD-TPS, %	1.0	0.7 – 1.4	1.1	0.8 – 1.6	0.036
Mean SD-TPS _{preA^l} , ms	795.3	692.4 - 884.9	846.7	760.6 - 967.4	0.046
SD-TPS _{preA^l} , %	4.6	3.0 – 8.6	3.7	2.9 – 5.4	0.227
Log - SD-TPS _{preA^l} , %	1.5	1.1 – 2.2	1.3	1.1 – 1.7	0.177
LGE extent (% LA surface)	11.6	6.0 – 17.6	13.8	7.6 – 28.4	0.061
Log LGE extent (% LA surface)	2.4	1.8 – 2.9	2.6	2.0 – 3.3	0.061

Data are presented as median (interquartile range [IQR]) or mean ± standard deviation (SD). CI: confidence interval; LAEF: LA emptying fraction; S_{max}^l: maximum longitudinal LA strain; SR: peak longitudinal strain rate; SR_e: early diastolic strain rate; SR_a: late diastolic strain rate; LVEF: left ventricular ejection fraction; TPS: time to peak strain; TPS_{preA^l}: time to peak pre-atrial contraction strain; LGE: late gadolinium enhancement.

Table 3 – Univariable and multivariable analyses

	Model 1 Unadjusted		Model 2 Clinical variables		Model 3 Model 2 + V _{min} + S _{max}	
	β	p	β	p	β	p
Log SD-TPS, %	0.66	< 0.001	0.57	0.001	0.60	0.001
Log SD-TPS _{preA^l} , %	0.19	0.034	0.21	0.020	0.18	0.045

Model 2, adjusted for age, sex, type of atrial fibrillation, body mass index, history of cardiac failure, hypertension, obstructive sleep apnea. Model 3, covariables included in Model 2 in addition to minimum left atrial volume and maximum longitudinal strain. V_{min}: minimum left atrial volume; S_{max}: maximum longitudinal strain; SD: standard deviation; TPS: time to peak strain; TPS_{preA^l}: time to peak pre-atrial contraction strain.

obstructive sleep apnea, hypertension, V_{min}^l, and S_{max}^l both indices SD-TPS and SD-TPS_{preA^l} remained significantly associated with LA-LGE (SD-TPS, β: 0.60, p = 0.001; SD-TPS_{preA^l}, β: 0.18, p = 0.045) (Table 3). Figure 4 displays the relationship between LA-LGE and LA intra-atrial dyssynchrony. There was no significant multiplicative interaction between AF type and LA intra-atrial dyssynchrony (interaction term for SD-TPS: 0.008, p = 0.258 and SD-TPS_{preA^l}: 0.003, p = 0.158). The LA-LGE analysis was performed in a consistent manner in all cases and took 60 ± 20 minutes per case, also depending on the image quality.

Dyssynchrony: inter-reader and intra-reader reproducibility

Interobserver and intraobserver variabilities of LA analysis for the MTT method were assessed in 15 randomly select subjects (Table 4, Figure 5). All parameters showed excellent intraobserver reproducibility (ICC 0.86 and 0.85 for SD-TPS and SD-TPS_{preA^l} respectively, p < 0.001) (Figure 5) without significant systematic bias. In addition, both parameters showed good to excellent interobserver reproducibility (ICC 0.86 and 0.74 for SD-TPS and SD-TPS_{preA^l} respectively, p < 0.001) (Figure 5).

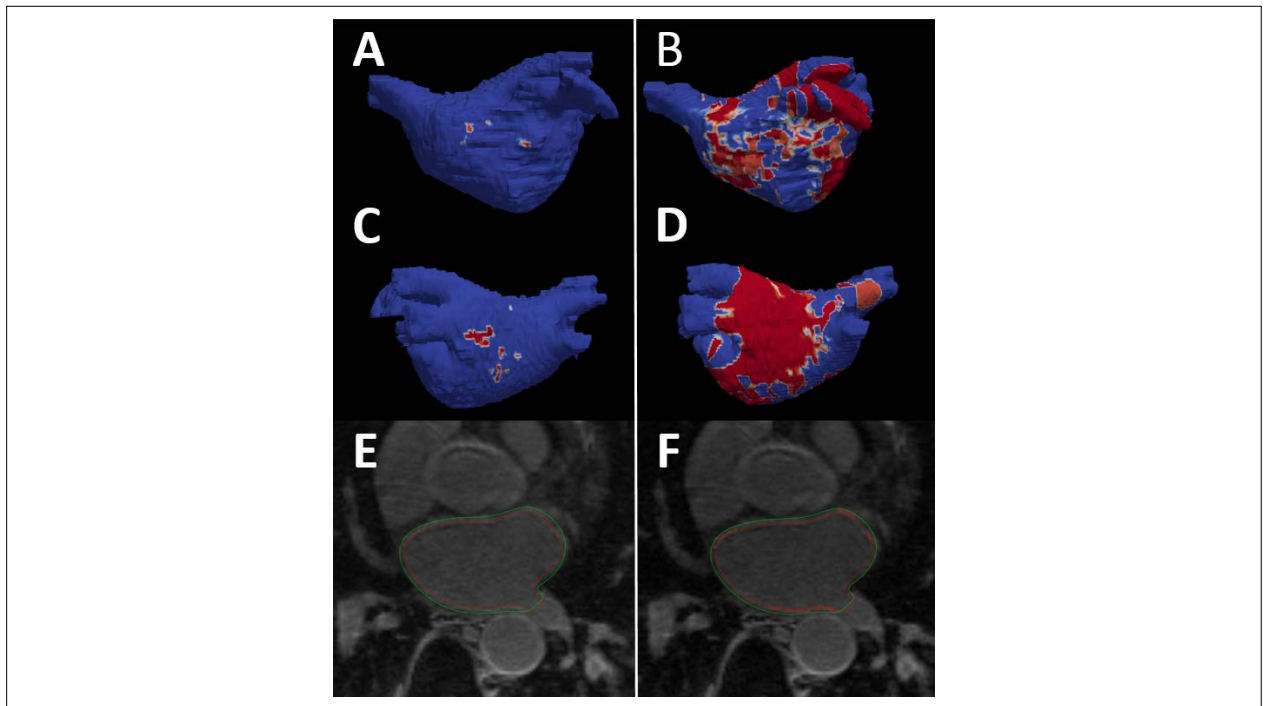


Figure 3 – Left atrial (LA) late gadolinium enhancement cardiac magnetic resonance (CMR). A – B: anterior LA shell view with areas of enhancement (red). C – D: posterior LA shell view with areas of enhancement (red). E – F: quantification of LA enhancement by CMR using image intensity ratio (IIR). Left side (A, C, and E), individual with low enhancement – right side (B, D, and F), individual with high enhancement.

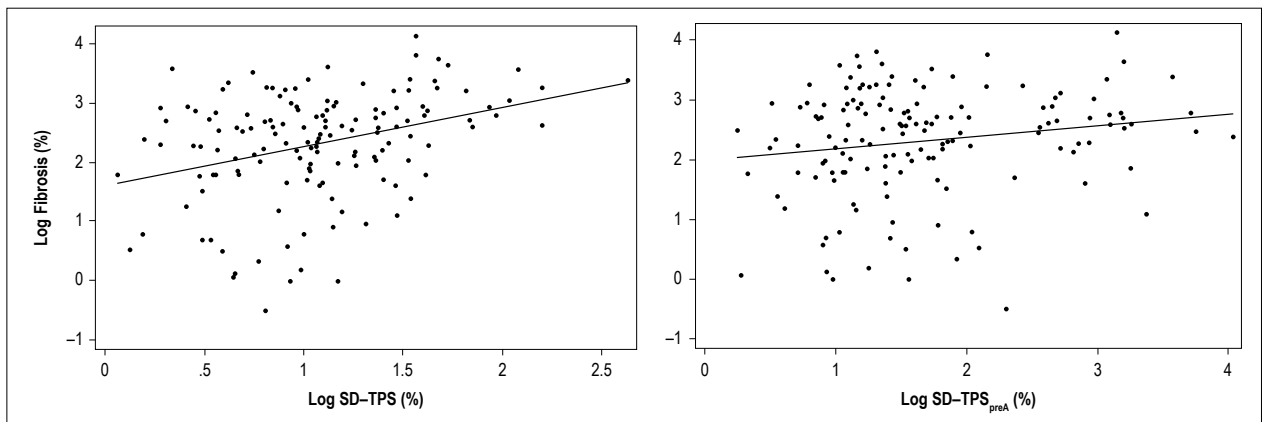


Figure 4 – Association between left atrial (LA) intra-atrial dyssynchrony and LA late gadolinium enhancement (LA-LGE). A, regression between LA-LGE and the standard deviation of the time to peak strain (SD-TPS); B, regression between LA-LGE and the standard deviation of the time to peak pre-atrial strain (SD-TPS_{preA}). Blue line, linear regression line. Log: logarithmically transformed variables; SD: standard deviation.

Discussion

The main findings are summarized as follows: 1) LA intra-atrial dyssynchrony was independently associated with LA-LGE, 2) LA intra-atrial dyssynchrony was significantly greater in patients with persistent AF than in those with paroxysmal AF, 3) LA intra-atrial dyssynchrony is a reproducible index, and 4) LA intra-atrial dyssynchrony analysis is less time-consuming than LA-LGE.

LA-LGE and dyssynchrony

Our multivariable analysis showed that LA intra-atrial dyssynchrony is associated with LA-LGE after adjusting for clinical risk factors including the AF type. This finding serves as evidence to the potential use of LA intra-atrial dyssynchrony as a surrogate for LA-LGE. In addition, our analysis showed that patients with persistent AF had significantly greater LA intra-atrial dyssynchrony than those with paroxysmal AF. In contrast, there

Table 4 – Inter-reader and intra-reader reproducibility of the left atrial measurements. Results are reported as mean ± standard deviation

LA parameter	Inter-reader		ICC	p
	Difference (mean ± SD)			
SD-TPS, %	-0.05 ± 0.21		0.86	< 0.001
SD-TPS _{preA} , %	-0.09 ± 0.83		0.74	< 0.001
LA parameter	Intra-reader		ICC	p
	Difference (mean ± SD)			
SD-TPS, %	0 ± 0.25		0.86	< 0.001
SD-TPS _{preA} , %	-0.03 ± 0.73		0.85	< 0.001

LA: left atrial; SD: standard deviation; ICC: intraclass correlation coefficient; TPS: time to peak strain; TPS_{preA}: time to peak pre-atrial contraction strain.

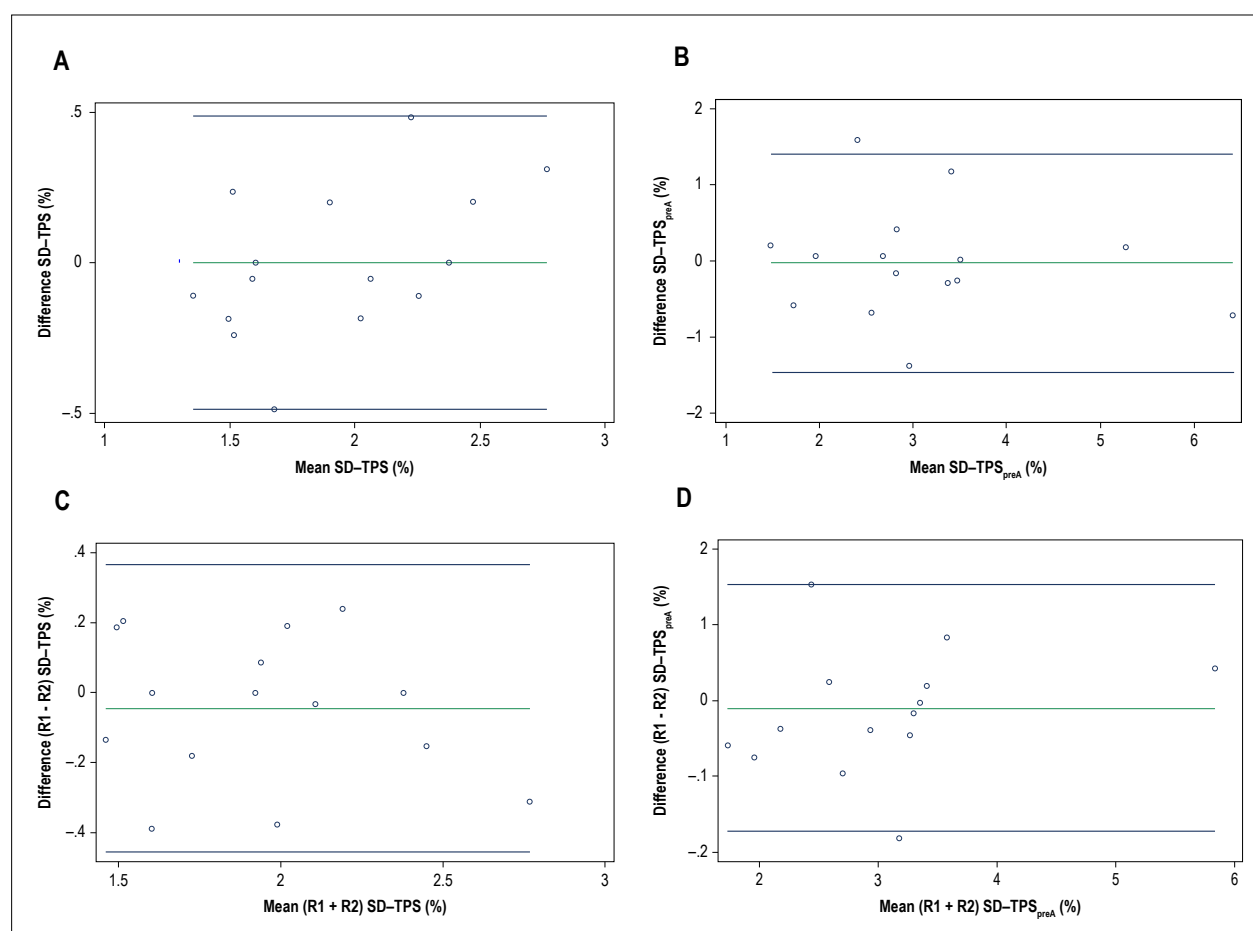


Figure 5 – Intra-reader and inter-reader reproducibility – Bland-Altman plot. A, standard deviation of the time to peak strain (SD-TPS) intra-reader reproducibility. B, standard deviation of the time to peak pre-atrial strain (SD-TPS_{preA}) intra-reader reproducibility. C, SD-TPS inter-reader reproducibility. D, SD-TPS_{preA} inter-reader reproducibility. R1: first reader; R2: second reader.

was no significant difference in LA-LGE between patients with persistent and paroxysmal AF, although there was a trend for a larger extent of LA-LGE with persistent AF. A possible explanation to account for these results is that intra-atrial dyssynchrony likely reflects subtle changes in atrial architecture that could generate AF but is not captured by LGE or other indices of LA function. In fact, mechanical dyssynchrony was a more specific

marker of AF recurrence after AF ablation when compared to LA scar and function (8). Technical difficulties associated with LA-LGE acquisition and processing may also account for the finding. For example, the thin wall of the LA (~3 mm) poses a challenge to the spatial resolution of CMR. In addition, only a small fraction of intravenously administered contrast perfuses the LA wall because the vast majority perfuses the ventricles

via the coronary arteries. Our result also showed that the LA intra-atrial dyssynchrony analysis is less time-consuming (5 ± 9 minutes) than LA-LGE (60 ± 20 minutes). This finding suggests that the implementation of LA intra-atrial dyssynchrony analysis in routine clinical practice would not significantly impede the clinical workflow of preprocedural assessment. The possibility that cardioversion-induced atrial stunning could have confounded our findings is low because: 1) cardioversion was performed in only a minority of patients in both groups and 2) there was no significant difference in the fraction of patients who underwent cardioversion between both groups.

LA dyssynchrony reproducibility

Our results showed excellent intra-reader reproducibility of LA intra-atrial dyssynchrony, with ICC ranging from 0.74 to 0.86 for SD-TPS, and 0.85 to 0.95 for SD-TPS_{preAF}, with the mean difference of 0 and -0.03, respectively (Table 4, Figure 5). The inter-reader reproducibility was also excellent to good, with ICC ranging from 0.86 for SD-TPS and 0.74 for SD-TPS_{preAF} with the mean difference of -0.05 and -0.09, respectively (Table 4, Figure 5). Both intra-reader and inter-reader reproducibility were similar to the values described in studies using 2D and 3D echocardiography.¹⁷

Limitations

This study accounts for a single-center, retrospective, cross-sectional analysis of patients referred for PVI to treat drug-refractory AF in a tertiary center. Therefore, there is a non-negligible chance of selection bias. For the dyssynchrony analysis, we used only two- and four-chamber cine CMR, which was included in a routine image-acquisition protocol. Therefore, it is possible that our analysis underestimated the degree of dyssynchrony by missing regions that were not covered by those two views. Since the strain was 2D and was obtained only in the in-plane direction, the strain values may have been underestimated compared with those in 3D strains. Besides, the CMR temporal resolution may also explain our lower values of dyssynchrony compared to echocardiography.¹⁷ There is a chance of underestimation of dyssynchrony due to spontaneous restoration of sinus rhythm a few weeks before the CMR. However, we believe that this fact would happen more often in individuals with paroxysmal AF; thus, our findings may have underestimated the real difference in dyssynchrony between individuals with paroxysmal and persistent AF by underestimating the dyssynchrony in the paroxysmal group. Finally, we had to

exclude subjects who were not in sinus rhythm by the time of the cine image acquisition, which could be a limitation for the application of our method in subjects with persistent AF.

Conclusions

LA intra-atrial dyssynchrony is significantly associated with LA-LGE independent of traditional cardiovascular risk factors or LA structure and function. Moreover, LA intra-atrial dyssynchrony was greater in individuals with persistent AF than in those with paroxysmal AF, whereas LA-LGE was not significantly different between the two AF types. LA intra-atrial dyssynchrony is a reproducible index to quantify LA remodeling and is less time-consuming than LA-LGE. Intra-atrial dyssynchrony can be used as a surrogate for the underlying tissue remodeling in patients with AF.

Author contributions

Conception and design of the research: Ciuffo LA, Lima J, Ashikaga H; Acquisition of data na Statistical analysis: Ciuffo LA; Analysis and interpretation of the data: Ciuffo LA, Tao S; Obtaining financing: Ashikaga H; Writing of the manuscript: Ciuffo LA, Ashikaga H; Critical revision of the manuscript for intellectual content: Lima J, Balouch M, Tao S, Nazarian S, Marine JE, Calkins H, Ashikaga H, Vasconcellos HD, Spragg DD, Berger RD.

Potential Conflict of Interest

No potential conflict of interest relevant to this article was reported.

Sources of Funding

There were no external funding sources for this study.

Study Association

This study is not associated with any thesis or dissertation work.

Ethics approval and consent to participate

This study was approved by the Ethics Committee of The Johns Hopkins IRB under the protocol number CIR0004531. All the procedures in this study were in accordance with the 1975 Helsinki Declaration, updated in 2013. Informed consent was obtained from all participants included in the study.

References

1. Lip GYH, Brechin CM, Lane DA. The Global Burden of Atrial Fibrillation and Stroke. *Chest*. 2012;142(6):1489–98.
2. Wolf PA, Abbott RD, Kannel WB. Atrial fibrillation as an independent risk factor for stroke: the Framingham Study. *Stroke*. 1991;22(8):983–8.
3. Bunch TJ, Weiss JP, Crandall BG, May HT, Bair TL, Osborn JS, et al. Atrial fibrillation is independently associated with senile, vascular, and Alzheimer's dementia. *Hear Rhythm*. 2010;7(4):433–7.
4. Ganesan AN, Shipp NJ, Brooks AG, Kuklik P, Lau DH, Lim HS, et al. Long-term outcomes of catheter ablation of atrial fibrillation: a systematic review and meta-analysis. *J Am Heart Assoc*. 2013;2(2):1–14.
5. Khurram IM, Habibi M, Gucuk Ipek E, Chrispin J, Yang E, Fukumoto K, et al. Left Atrial LGE and Arrhythmia Recurrence Following Pulmonary Vein Isolation for Paroxysmal and Persistent AF. *JACC Cardiovasc Imaging*; 2016;9(2):142–8.
6. Marrouche NF, Wilber D, Hindricks G, Jais P, Akoum N, Marchlinski F, et al. Association of atrial tissue fibrosis identified by delayed enhancement MRI and atrial fibrillation catheter ablation: the DECAAF study. *JAMA*. 2014;311(5):498–506.
7. Calkins H, Hindricks G, Cappato R, Kim Y-H, Saad EB, Aguinaga L, et al. 2017 HRS/EHRA/ECAS/APHRs/SOLAECE expert consensus statement on catheter and surgical ablation of atrial fibrillation. *Hear Rhythm*; 2017;14(10):e275–444.
8. Ciuffo L, Tao S, Gucuk Ipek E, Zghaib T, Balouch M, Lima JAC, et al. Intra-Atrial Dysynchrony During Sinus Rhythm Predicts Recurrence After the First Catheter Ablation for Atrial Fibrillation. *JACC Cardiovasc Imaging*. 2019;12(2):310–9.
9. Zareian M, Ciuffo L, Habibi M, Opdahl A, Chamera EH, Wu CO, et al. Left atrial structure and functional quantitation using cardiovascular magnetic resonance and multimodality tissue tracking: validation and reproducibility assessment. *J Cardiovasc Magn Reson*. 2015 July 1;17:52.
10. Habibi M, Lima JAC, Khurram IM, Zimmerman SL, Zipunnikov V, Fukumoto K, et al. Association of left atrial function and left atrial enhancement in patients with atrial fibrillation: cardiac magnetic resonance study. *Circ Cardiovasc Imaging*. 2015;8(2):e002769.
11. Khurram IM, Beinart R, Zipunnikov V, Dewire J, Yarmohammadi H, Sasaki T, et al. Magnetic resonance image intensity ratio, a normalized measure to enable interpatient comparability of left atrial fibrosis. *Heart Rhythm*. 2014;11(1):85–92.
12. Harrison JL, Jensen HK, Peel SA, Chiribiri A, Grondal AK, Bloch LO, et al. Cardiac magnetic resonance and electroanatomical mapping of acute and chronic atrial ablation injury: a histological validation study. *Eur Heart J*. 2014; 35(22):1486–95.
13. Chrispin J, Ipek EG, Habibi M, Yang E, Spragg D, Marine JE, et al. Clinical predictors of cardiac magnetic resonance late gadolinium enhancement in patients with atrial fibrillation. *Eur Eur pacing, arrhythmias, Card Cell Electrophysiol*. 2017;19(3):371–7.
14. Inoue YY, Alissa A, Khurram IM, Fukumoto K, Habibi M, Venkatesh BA, et al. Quantitative tissue-tracking cardiac magnetic resonance (CMR) of left atrial deformation and the risk of stroke in patients with atrial fibrillation. *J Am Heart Assoc*. 2015;4(4):pii:e001844.
15. Mochizuki A, Yuda S, Oi Y, Kawamukai M, Nishida J, Kouzu H, et al. Assessment of left atrial deformation and synchrony by three-dimensional speckle-tracking echocardiography: comparative studies in healthy subjects and patients with atrial fibrillation. *J Am Soc Echocardiogr*. 2013; 26(2):165–74.
16. Dell'Era G, Rondano E, Franchi E, Marino PN. Atrial asynchrony and function before and after electrical cardioversion for persistent atrial fibrillation. *Eur J Echocardiogr*. 2010;11(7):577–83.
17. Habibi M, Chahal H, Opdahl A, Gjesdal O, Helle-Valle TM, Heckbert SR, et al. Association of CMR-measured LA function with heart failure development: results from the MESA study. *JACC Cardiovasc Imaging*. 2014;7(6):570–9.
18. Ujino K, Barnes ME, Cha SS, Langins AP, Bailey KR, Seward JB, et al. Two-dimensional echocardiographic methods for assessment of left atrial volume. *Am J Cardiol*. 2006;98(9):1185–8.
19. Nacif MS, Barranhas AD, Turkbey E, Marchiori E, Kawel N, Mello RAF, et al. Left atrial volume quantification using cardiac MRI in atrial fibrillation: comparison of the Simpson's method with biplane area-length, ellipse, and three-dimensional methods. *Diagn Interv Radiol*. 2013;19(3):213–20.
20. Haycock GB, Schwartz GJ, Wisotsky DH. Geometric method for measuring body surface area: a height-weight formula validated in infants, children, and adults. *J Pediatr*. 1978;93(1):62–6.
21. Ludbrook J. Linear regression analysis for comparing two measurers or methods of measurement: but which regression? *Clin Exp Pharmacol Physiol*. 2010;37(7):692–9.
22. Bland JM, Altman DG. Statistical methods for assessing agreement between two methods of clinical measurement. *Lancet*. 1986;1(8476):307–10.



This is an open-access article distributed under the terms of the Creative Commons Attribution License